Cement and Concrete Research 41 (2011) 9–19

Contents lists available at ScienceDirect

Cement and Concrete Research

journal homepage: http://ees.elsevier.com/CEMCON/default.asp

Effect of crack width on chloride diffusion coefficients of concrete by steady-state migration tests

Seung Yup Jang [a], Bo Sung Kim [b], Byung Hwan Oh [c,*]

[a] Korea Railroad Research Institute, 360-1, Worram-dong, Uiwang, Gyeonggi-do 437-757, Republic of Korea
[b] Korea Land and Housing Corporation, 217, Jungja-dong, Seoungnam, Gyeonggi-do 463-755, Republic of Korea
[c] Seoul National University, Shinrim-dong, Gwanak-ku, Seoul 151-742, Seoul, Republic of Korea

ARTICLE INFO

Article history:
Received 25 April 2010
Accepted 31 August 2010

Keywords:
Concrete (E)
Crack width (B)
Diffusion coefficient (C)
Durability (C)
Migration test (C)

ABSTRACT

The purpose of the present study is to explore the diffusion characteristics of cracked concrete according to the width of cracks. Major test variables include crack width, concrete strength, fly ash addition, and maximum aggregate size. The diffusion characteristics have been measured by steady-state migration test. The present study indicates that the diffusion coefficients do not increase with increasing crack widths up to the so-called "threshold crack width." The threshold crack width for diffusion is found to be around 55–80 μm. Above this threshold value, the diffusion coefficients start to increase with crack width. A composite model with the introduction of "crack geometry factor" was derived to identify the diffusion coefficient in cracked concrete. It was shown that the crack geometry factor ranges from 0.067 to 0.206. Finally, the effects of concrete strength, fly ash addition and maximum aggregate size on diffusion coefficients are also discussed.

1. Introduction

Corrosion of steel reinforcement in concrete due to chloride ions is one of the major causes of deterioration of concrete structures in marine environment or subjected to deicing salts. Thus, the prediction of chloride penetration into concrete has been an important issue in the design of concrete structures for the last several decades, and studied by a number of investigators [1–10]. However, the previous researches have been mostly focused on the chloride transport in sound uncracked concrete. On the other hand, cracks are inevitable in most concrete members due to the weakness of concrete in tension and these cracks may affect greatly the diffusivity of chloride in concrete. Therefore, the effect of cracks on chloride transport must be considered realistically for more reliable design of concrete structures especially under chloride environment. Furthermore, to make more economical and reliable structures, the performance-based design is strongly requested recently. To cope with this request in design, the accurate prediction of the performance of structures is an essential task. If the effect of cracks is not considered realistically in the durability design, the performance and service life of concrete structures may be overestimated which may lead to an unexpected premature failure of structures.

In this paper, therefore, the diffusion coefficients of cracked concrete have been studied to clarify the change of diffusion coefficients according to crack width. The steady-state migration test was employed to measure the diffusion coefficients. Crack width was selected as a main test variable, and a crack of desired width was induced by the controlled split test in the laboratory. Based on the test data, the relationship between crack width and diffusion coefficient is analyzed. The compressive strength of concrete, addition of fly ash and maximum aggregate size were also chosen as test variables in order to explore the effects of these parameters on the diffusion of cracked concrete.

2. Review of previous researches

The effects of crack on transport properties have been studied by several researchers [11–18]. According to Gérard et al. [15], the permeability can be highly increased over 100 times by damage of concrete. The transport properties of cracked concrete may be estimated based on the damage or fracture mechanics, if the quantitative relationship between the transport properties and the cracking of concrete can be established. Some researchers have tried to correlate the transport properties of cracked concrete to the loading level or tensile stress of concrete [19–21], or to the inelastic strain of concrete [15]. However, it is difficult to obtain the quantitative relationship between the loading level, tensile stress or tensile strain and the transport properties because the characteristics of cracking becomes different according to the types of loading such as tension, compression, flexure and combined loadings. Therefore it seems more appropriate to directly correlate the transport properties and the crack width.

Wang et al. [18] and Aldea et al. [11,12] have tried to relate the permeability directly to the crack width measured from the feedback

* Corresponding author. Tel.: +82 11 304 9547.
E-mail address: bhohcon@snu.ac.kr (B.H. Oh).

0008-8846/$ – see front matter © 2010 Elsevier Ltd. All rights reserved.
doi:10.1016/j.cemconres.2010.08.018

controlled splitting test, followed by the conventional water permeability test. Wang et al. [18] argue that a crack opening displacement (COD) smaller than 50 μm under loading (≈15 μm after unloading) rarely affects the permeability. However, when a COD is increased from 50 to 200 μm under loading (≈15 to 65 μm after unloading), the permeability increases rapidly. Over 200 μm (65 μm after unloading), it shows a steady increase. Aldea et al. [11,12] also report similar results.

On the other hand, it appears that the quantitative relationship between crack and diffusion is not clearly established yet. Aldea et al. [12] have reported that the diffusion is less sensitive to the crack width. They argue that this is due to the fact that the diffusion is proportional to the crack width [22], while the permeation is proportional to the cube of the crack width [23].

Several authors persist that there is a certain value of crack width that the crack becomes first connected [13,18]. This is here denoted as the "threshold crack width." Below the threshold crack width, cracks have little influence on transport, mainly because of the self-healing effects inside cracks [13,17]. Gagné et al. [13] also support this "threshold crack width" by reporting that the crack can act as a continuous channel when the crack width exceeds about 55 μm. According to Wang et al. [18], this threshold crack width for water permeation is around 15 μm (after unloading). It is worth noting that this range of threshold crack width is generally less than the allowable limit of crack width for prestressed concrete in CEB-FIP Model Code 90 [24] in which the allowable limit value is prescribed as 200 μm to prevent the depassivation of steel reinforcement.

3. Diffusion in cracked concrete — a hypothetical parallel model

To establish a quantitative relationship between crack width and diffusivity of concrete which is similar with an analogy to the relationship between diffusion and pore structure of hardened cement paste [25], the diffusion coefficient in a single crack is defined as

$$D_{cr} = \beta_{cr} D_0 \tag{1}$$

where β_{cr} is defined here as the "crack geometry factor" accounting for tortuousness, connectivity and constrictivity of the crack path perpendicular to the flow direction, and D_{cr} and D_0 are the diffusion coefficients of chloride ions at crack and in free solution [m^2/s], respectively. In other words, crack is considered as a straight channel with diffusion coefficient of $D_{cr}=\beta_{cr}D_0$ as shown in Fig. 1. Here the crack geometry factor β_{cr} is a reciprocal of the tortuosity suggested by Gérard et al. [16]. At 25 °C, D_0 is 2.032×10^{-5} cm^2/s [26].

On steady-state regime, the cracked concrete can be depicted as a two-phase parallel model as shown in Fig. 2. Then, the total flux of chlorides J_{tot} can be given as follows [14]

$$J_{tot} = \frac{A_{uncr}J_{uncr} + A_{cr}J_{cr}}{A_{tot}} \tag{2}$$

where J_{cr} and J_{uncr} are the ionic fluxes in cracked and sound (uncracked) concrete [kg/m^2s], respectively, and A_{cr} and A_{uncr} are the cross-sectional areas of cracked and sound concrete [m^2], respectively. A_{tot} is the total cross-sectional area [m^2]. According to Fick's 1st law, at steady state, the ionic flux is described as

$$D_{eq}\nabla c = \frac{A_{uncr}}{A_{tot}}(D\nabla c) + \frac{A_{cr}}{A_{tot}}(D_{cr}\nabla c) \tag{3}$$

where D_{eq} is the equivalent diffusion coefficient of cracked concrete [m^2/s], and D and D_{cr} are the diffusion coefficients of sound and cracked concrete [m^2/s], respectively. ∇c is the concentration gradient [kg/m^4]. Since $A_{uncr}/A_{tot}\approx 1$, Eq. (3) may be rewritten as

$$\frac{D_{eq}}{D} = 1 + \frac{A_{cr}}{A_{tot}}\frac{D_{cr}}{D} = 1 + a_{cr}\frac{D_0}{D} \tag{4}$$

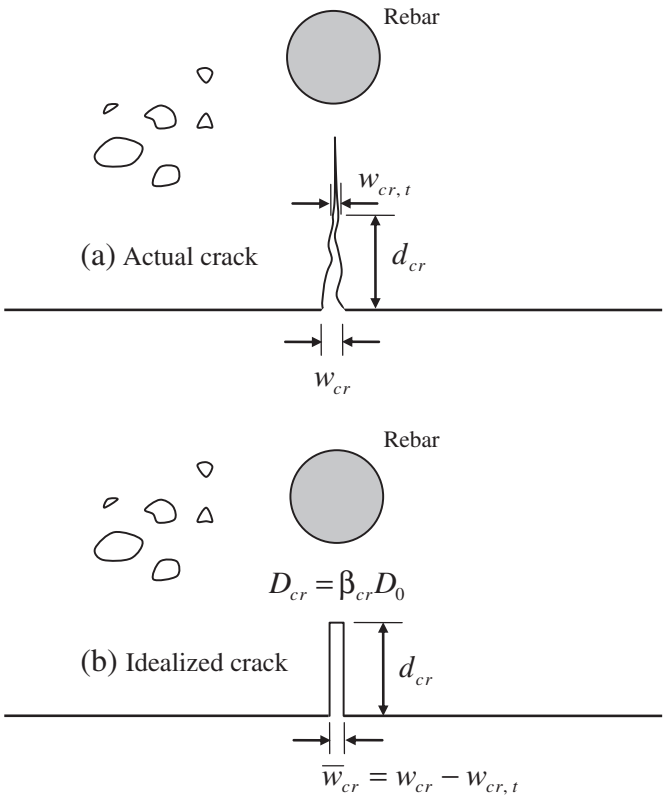

Fig. 1. Simplified crack model for diffusion.

where $a_{cr}=\beta_{cr}(A_{cr}/A_{tot})$. This implies that the relationship between crack width and D_{eq} is linear, which coincides with the derivation by Gérard and Marchand [14] for 1-D crack pattern. For cylindrical cross-section specimen, $A_{cr}/A_{tot}=4w_{cr}/(\pi d)$ where w_{cr} is the crack width [m] and d is the specimen diameter [m], and then Eq. (4) may be written as follows.

$$\frac{D_{eq}}{D} = 1 + \frac{4w_{cr}\beta_{cr}}{\pi d}\frac{D_0}{D} \tag{5}$$

If one assumes reasonably that there exists a certain "threshold crack width" under which the crack doses not affect the diffusion of

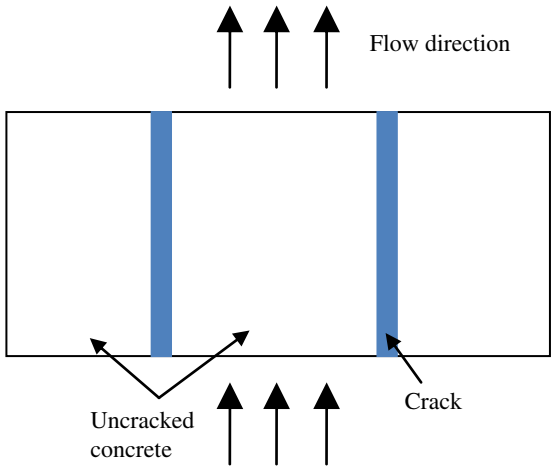

Fig. 2. Two-phase parallel model for diffusion in cracked concrete.

Table 1
Test variables and mixture proportions.

Specimen ID	Compressive strength [MPa]	Max. agg. size [mm]	Water-binder ratio	Mixture proportions				
				Water [kg/m^3]	Cement [kg/m^3]	Fly ash [kg/m^3]	Sand [kg/m^3]	Gravel [kg/m^3]
S15	15.68	25	0.64	187	292	–	775	999
S21	22.54	25	0.53	187	353	–	716	1009
S30	31.36	25	0.40	176	440	–	671	1010
S30F20	34.30	25	0.40	176	352	88	671	1010
S30G13	31.40	13	0.40	204	509	–	746	803

Table 2
Chemical compositions of cement and fly ash.

Type	CaO	SiO_2	Al_2O_3	Fe_2O_3	MgO	K_2O	Na_2O	SO_3	LOI[a]
Cement(OPC)	61.20	22.00	6.20	3.20	2.80	1.10	0.10	2.00	1.40
Fly ash	3.89	59.74	23.60	6.07	0.95	0.96	0.49	0.40	3.90

[a] Loss on ignition.

chloride ions as reported in the previous studies [11–13,17,18], Eq. (5) can be rewritten as

$$\frac{D_{eq}}{D} = 1 + \frac{4\overline{w}_{cr}\beta_{cr}}{\pi d}\frac{D_0}{D} \tag{6}$$

where $\overline{w}_{cr}$ is the equivalent crack width [m], $\overline{w}_{cr} = w_{cr} - w_{cr,t}$ when the threshold crack width is defined as $w_{cr,t}$.

4. Experimental program

4.1. Test variables and mixture proportions

The main test variable in this study is the crack width at unloaded state. This is to find out the effect of crack width on the diffusion. The crack widths were selected ranging from 0 to 200 μm. The other test variables include compressive strength, addition of fly ash and maximum aggregate size in order to explore the effects of these parameters on the diffusion coefficients of cracked concretes. The mixture proportions according to test variables are shown in Table 1.

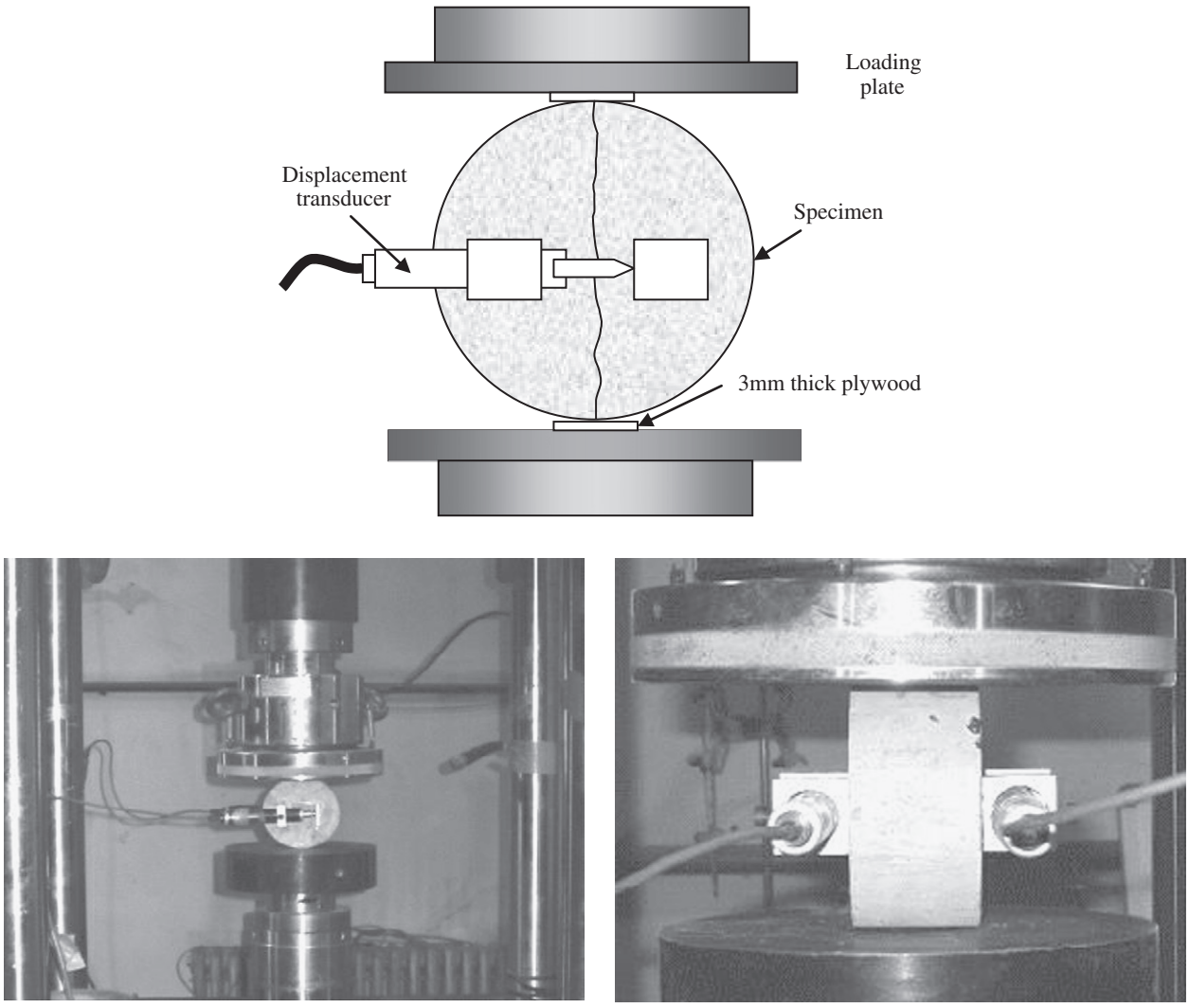

Fig. 3. Schematics and test set-up of crack width-controlled split test.

For all mixtures, the ordinary Portland cement (OPC) was used, and F-class fly ash was used for S30F20 test series. The target compressive strengths of concrete were 15 MPa (S15), 21 Mpa (S21), 30 MPa (S30), respectively (see Table 1). The maximum aggregate size was 25 mm except for one case, i.e., S30G13 as shown in Table 1 where the maximum aggregate size was 13 mm. The slump and air content are 15 cm and 4.5%, respectively. The chemical compositions of cement and fly ash are summarized in Table 2.

4.2. Induction of cracks by crack width-controlled split test

Ø100×200 mm cylindrical specimens were manufactured, and 50 mm-thick slices have been cut from the center parts of the specimens at 28 days after placement. The crack width-controlled split tests for inducing cracks in test specimens were performed (Fig. 3). First of all, two displacement transducers were installed on both cutting faces of test slices, and the test slices were loaded with the loading actuator at constant speed of 0.67 μm/s (see Fig. 3). When the average of two crack opening displacements (CODs) measured at both sides reached a certain specified value, the test specimens were unloaded automatically. Between the loading plate and the specimen, a piece of plywood was placed to prevent the fracture of specimens due to the local stress underneath the loading plate.

Since the crack closes to a certain extent after unloading, it is difficult to predict the crack width at unloaded state. Thus, repetitive tests were performed to obtain the relationship between the crack widths at loaded and unloaded states. Finally, crack widths of approximately 15, 30, 60, 80, 110, 150 and 200 μm have been obtained at unloaded state.

4.3. Measurement of diffusion coefficients by steady-state migration test

In this study, the steady-state migration test [6,10] was adopted to measure the diffusion coefficients as shown in Fig. 4. The diffusion coefficients from the steady-state migration test can be calculated from Nernst–Planck equation as follows [5]:

$$J_c = -D\frac{\partial c}{\partial x} + \frac{zF}{RT}Dc\frac{\partial U}{\partial x} \tag{7}$$

where J_c is the ionic flux at steady state [kg/m^{2}s], R is the gas constant (=8.3145 J/mol K), T is the absolute temperature [K], L is the specimen thickness [m], z is the ionic valence, F is the Faraday constant (=96,485 C per equivalent), U is the electrical potential measured [V]. Since the diffusive flux $-D\partial c/\partial x$ is very small compared with the migration flux, it is reasonably assumed as $-D\partial c/\partial x \approx 0$. Then, one may write from Eq. (7) as

$$D_{ssm} = \frac{RTL}{zFU}\frac{J_c}{c_1} \tag{8}$$

where c_1 is the chloride concentration in the upstream cell (catholyte). Here the flux of chloride ions J_c can be determined by the following relationship

$$J_c = \frac{V}{A}\left|\frac{\Delta c}{\Delta t}\right| \tag{9}$$

where V is the volume of the cell, A is the cross-sectional area which ions pass through and $\Delta c/\Delta t$ is the rate of chloride concentration change (increase or decrease), which can be obtained in the downstream cell (anolyte) or in the upstream cell (catholyte).

Truc et al. [10] report that it is more efficient and accurate to measure the rate of chloride concentration change in the upstream cell because it is not necessary to wait for the steady state in the upstream cell and, therefore, the problems related to the chemical reactions at the anode can be evitable. If we measure the rate of chloride concentration change in the upstream cell, then Eq. (8) is simply written as

$$D_{ssm} = \frac{RTL}{zFU}\frac{V}{A}\frac{1}{c_1}\left|\frac{\Delta c_1}{\Delta t}\right| = \frac{RTL}{zFU}\frac{V}{A}\left|\frac{\Delta(\ln c_1)}{\Delta t}\right| \tag{10}$$

As one can find from the above equations, only the concentration drops in the upstream cell are to be measured for determining diffusion coefficients.

On the other hand, even if the rate of chloride concentration change is measured in the downstream cell, the chloride concentration in the upstream cell c_1 should be measured during the test, and the average value after the steady state is reached is used in the calculation of the diffusion coefficient.

The chloride concentrations were determined using Ag–AgCl electrode. Since the exact titration takes too much time, only the potentials were measured by Ag–AgCl electrode during the test and the chloride concentrations were determined based on the potential–concentration curves that are obtained from chloride solutions of known concentrations.

The electrical potential was measured from the electric circuit (see Fig. 4). The potential supplied was 12 V, but the measured potential was dropped to about 9.8 V. In the calculation of the diffusion coefficients, 9.8 V is used. Two specimens for each test variable were tested to measure the diffusion coefficients.

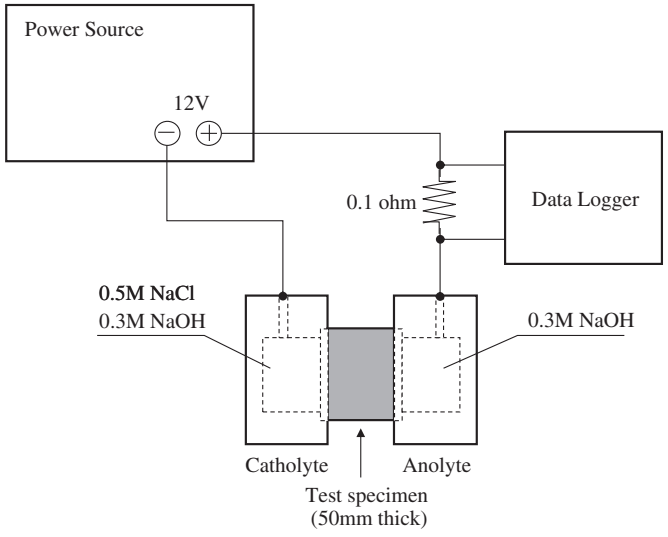

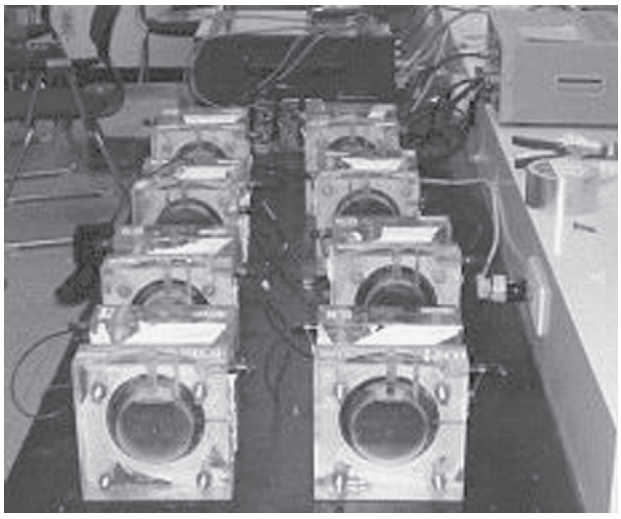

Fig. 4. Steady-state migration test set-up.

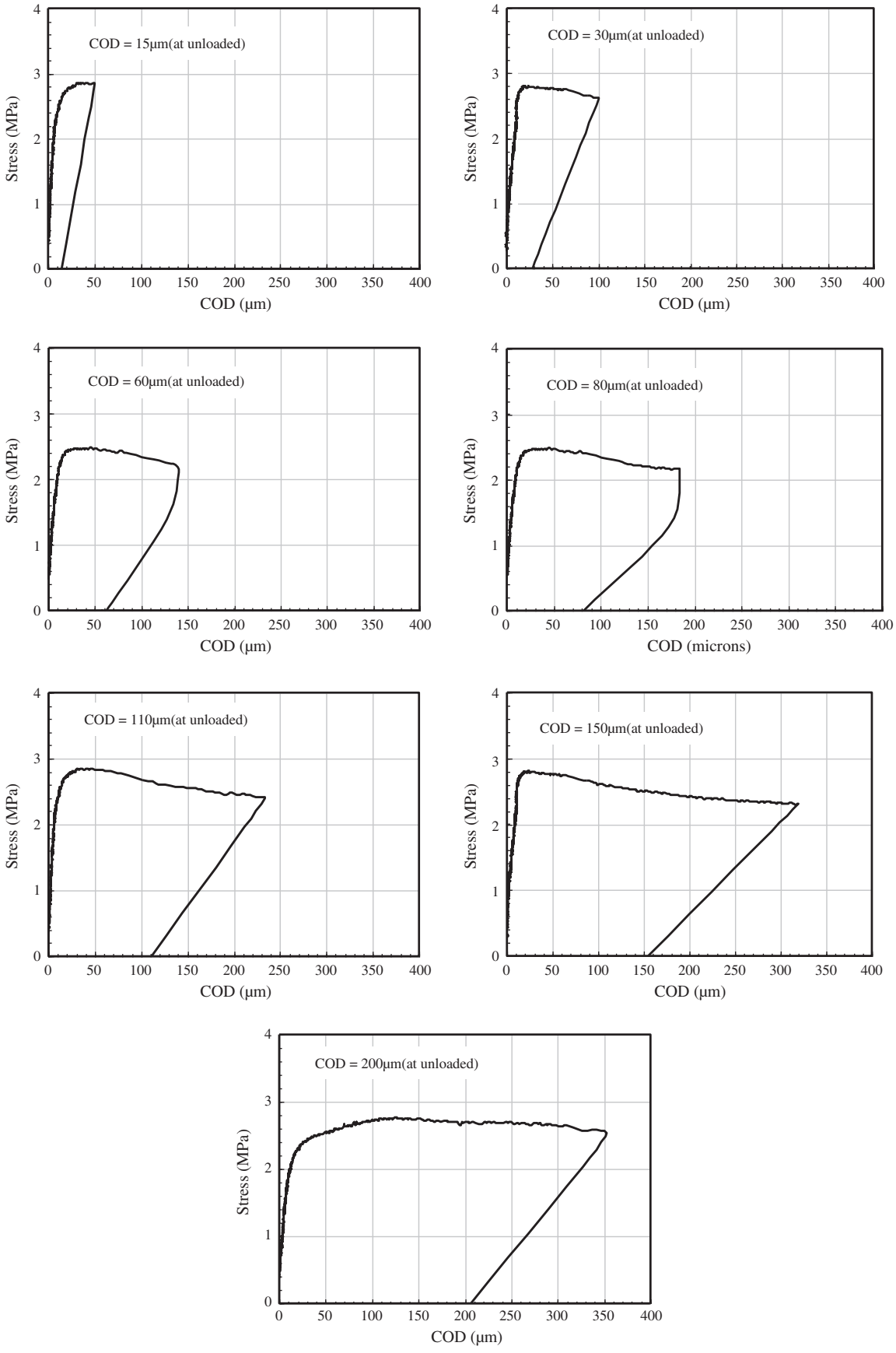

Fig. 5. Tensile stress–COD curves according to maximum CODs (test series S30).

5. Results and discussions

5.1. Results of crack width-controlled split test

Figs. 5 and 6 show the relationship between tensile stress and crack opening displacement (COD) obtained from the split tension test. The maximum tensile stress is mostly obtained at the COD of around 25–50 μm. After the tensile stress reaches its maximum, the stress decreases slowly with increasing COD values. When the target COD value was reached, the specimen was completely unloaded. Then, the COD at zero stress was measured with the reduction of COD values. As shown in Figs. 5 and 6, the slope of the unloading curve is less steep than that of loading curve, which indicates a reduction of stiffness of specimen caused by cracking. It is also found that the larger the crack width at loading state, the smaller the slope of the stress–COD curve.

Fig. 6 shows the relationship between split tensile stress and crack opening displacement (COD) according to the strength levels and mixture characteristics. It can be seen that the split tensile strengths are increased with increasing compressive strengths, but the CODs after unloading are not affected by concrete strength up to the strength level of at least 30 MPa. Also, the maximum aggregate size and addition of fly ash affect the split tensile strength, but not significantly the CODs after unloading (see Fig. 6).

Fig. 7 demonstrates that the recovery of crack width after unloading increases almost linearly with the increase of maximum CODs at loaded state up to about 300 μm. After this value, however, the recovery of crack width after unloading starts to decrease.

5.2. Rates of chloride concentration change and diffusion coefficients

Fig. 8 shows the variation of chloride concentration with time in the upstream and the downstream cells for S30 specimens (OPC concrete of 30 MPa strength) according to different crack widths. Fig. 8 indicates that when it reaches the steady state, the rate of chloride concentration increase or decrease becomes almost constant in the upstream and downstream cells. With these rates of chloride concentration change, $\Delta c/\Delta t$, in the steady state, the diffusion coefficients can be calculated based on the Eqs. (8)–(10). In a few specimens, a concentration drop was observed in the downstream cell, as shown in Fig. 8, which may be attributed to the chemical reactions that occurred at the anode [10]. Fig. 9 also shows the variation of chloride concentration with time in the upstream and the downstream cells according to the different concrete strengths, fly ash addition and different maximum aggregate size. It can be seen from Fig. 9 that the slope of concentration change becomes smaller as the concrete strength increases.

The measured rates of chloride concentration change and calculated diffusion coefficients are summarized in Table 3. The data in Table 3 exhibit that the rates of chloride concentration change obtained in the upstream and downstream cells are almost same each other except for S15 case. The S15 test series represents very low strength concrete ($f_c \approx 15$ MPa) and thus may exhibit larger variability in diffusion characteristics.

In Fig. 10, the diffusion coefficients obtained from the upstream and downstream cell data are compared. It is seen from Fig. 10 that the diffusion coefficients obtained from both upstream and downstream cells indicate good correlation. This suggests that the diffusion coefficients can be determined with almost same accuracy from the rates of chloride concentration change obtained either in the upstream cell or in the downstream cell. On the other hand, as Turc et al. [10] reported, the rate of chloride concentration drop can be obtained more quickly if one uses the upstream cell data. This may be confirmed from Fig. 8 or 9. As shown in Figs. 8 and 9, it takes about almost 500 h or more to reach the steady state in the downstream cell, while the rates of chloride concentration drop in the upstream cell become constant after around 200 h. Therefore, it can be said that it is more efficient and economical to use the upstream cell data to measure the diffusion coefficients, without loosing the accuracy in the measured data.

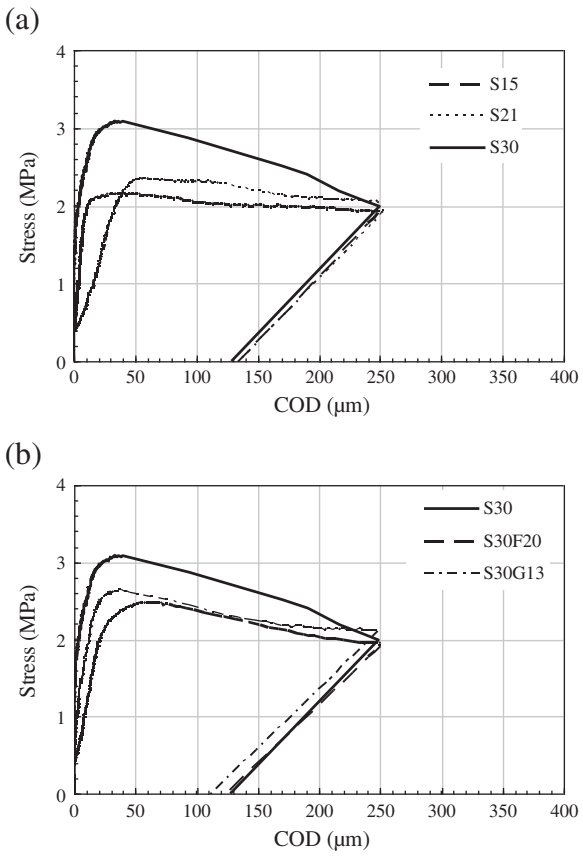

Fig. 6. Tensile stress–COD curves according to: (a) concrete strength, and (b) mixture characteristics.

5.3. Relationship between crack widths and diffusion coefficients

Fig. 11 demonstrates the relationship between diffusion coefficients and crack widths at unloaded state. As shown in Fig. 11, the diffusion coefficients do not increase with an increase of crack width up to about 80 μm. Over 80 μm in crack width, however, the diffusion coefficients start to increase. Thus, the crack width value of 80 μm may be called as the "threshold crack width" for diffusion. This value is a little bit higher than 15 μm for permeation found by Wang et al. [18]

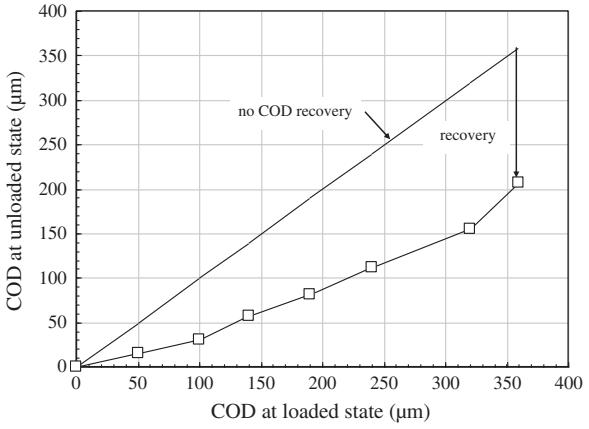

Fig. 7. Recovery of COD after unloading (test series S30).

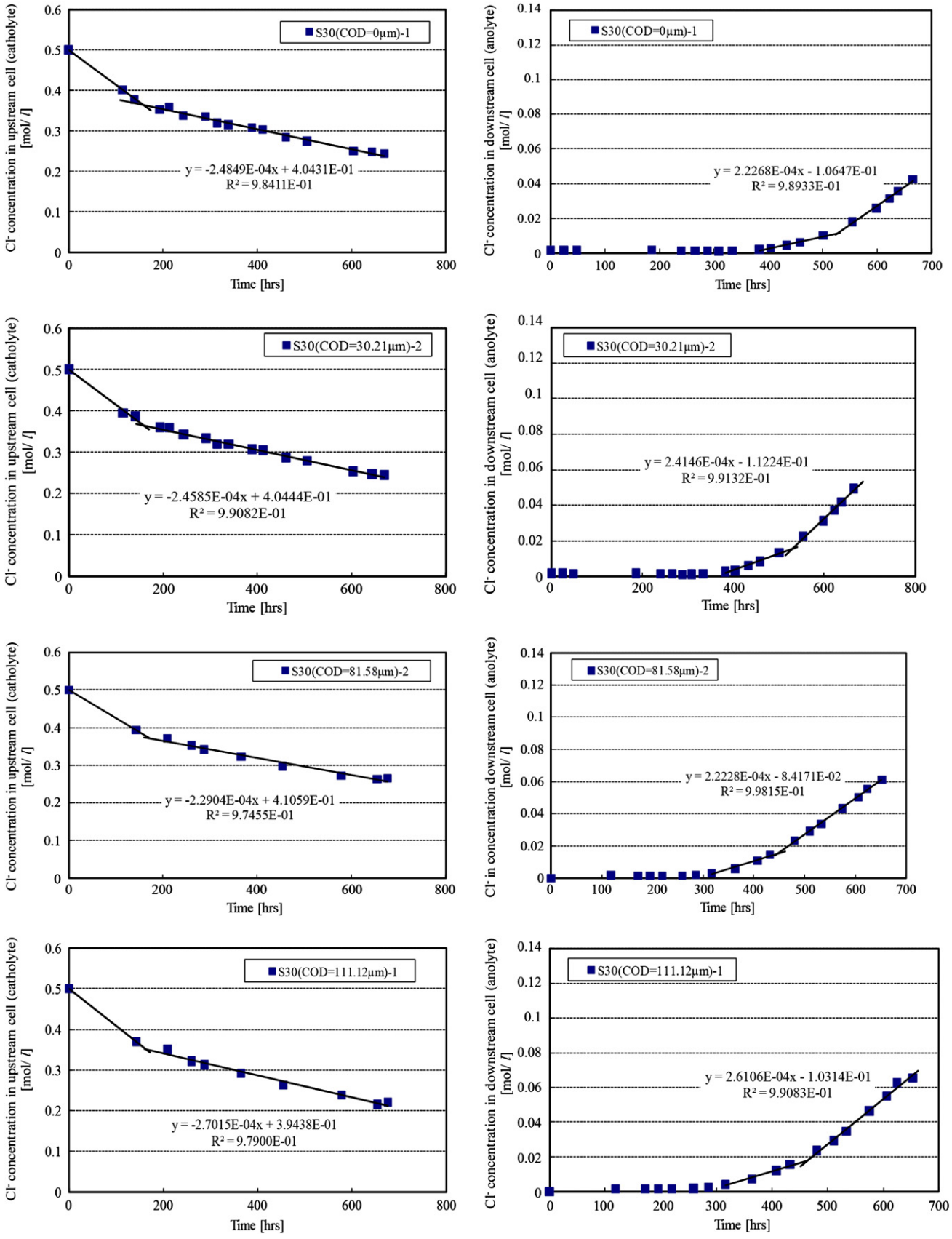

Fig. 8. Variation of chloride concentration in the upstream and downstream cells according to crack widths.

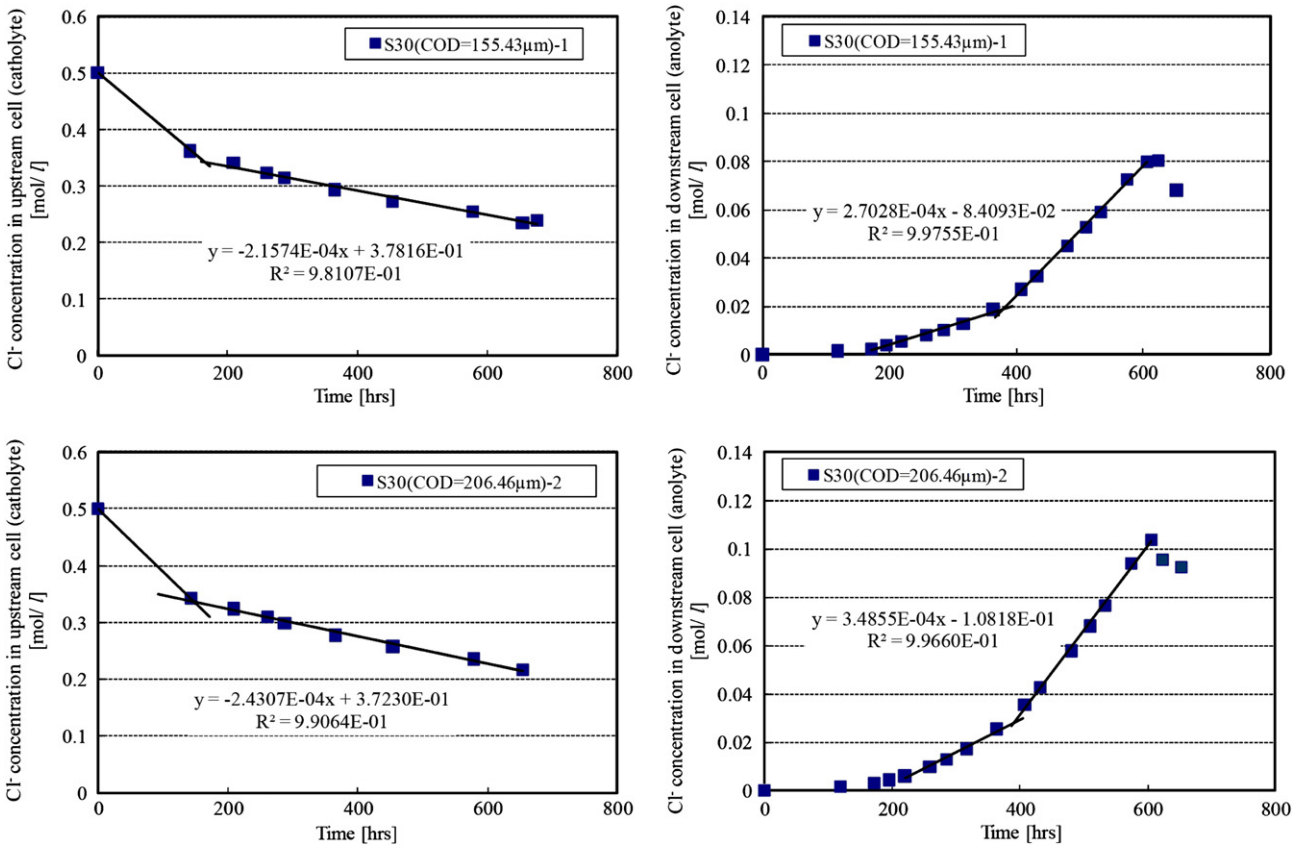

Fig. 8 (*continued*).

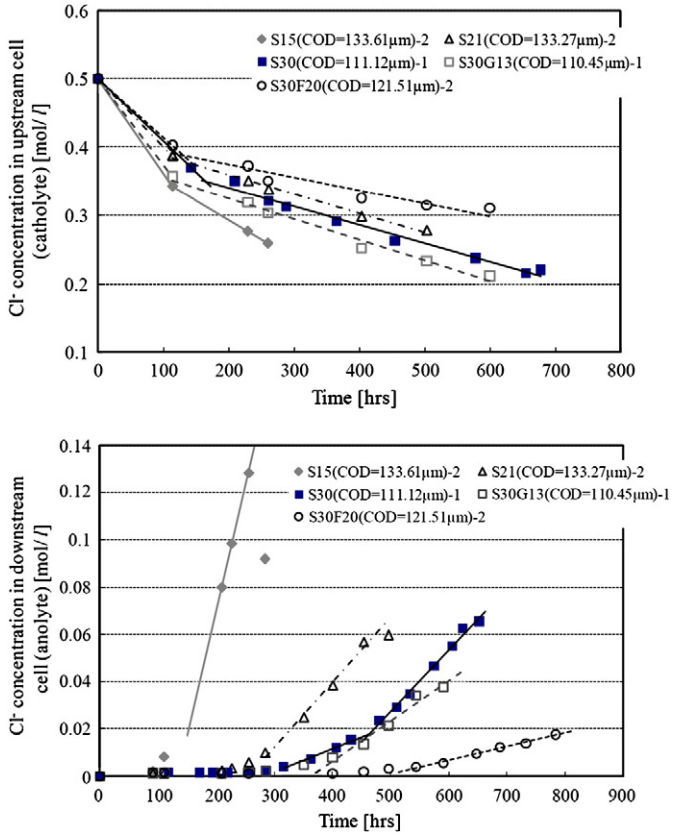

Fig. 9. Variation of chloride concentration in the upstream and downstream cells according to strength, fly ash addition and maximum aggregate size.

and 55 μm for diffusion suggested by Gagné et al. [13], but much closer to the latter. It may be therefore said that the threshold crack width for diffusion is higher than that for permeation and is around 55–80 μm based on these limited data.

Aldea et al. [11,12] did not directly measure the diffusion coefficients in their study, but measured the initial currents through the rapid chloride permeability test (RCPT) specified in ASTM C 1202 [27]. The relative diffusion coefficients can be estimated based on these initial current data by following Snyder's suggestion [8] that $D_{eq}/D \approx i_{eq}/i$ where $i_{eq}$is the initial current of cracked concrete and i is that of uncracked concrete. Fig. 12 shows the comparison of diffusion coefficients obtained from migration test and those estimated based on initial current data. Aldea et al. [12] suggest from their data that the diffusion is less affected by crack width up to the crack width of 200 μm for normal strength concrete as shown in see Fig. 12. On the other hand, the data obtained in this study reveal that the diffusion coefficients estimated from the initial current data also show an increase with increasing crack width, but this increase is observed only at around 200 μm crack width. The relative diffusivity at 200 μm crack width obtained from the initial current data is a little bit large compared to that obtained directly from chloride concentration data. This discrepancy is possibly due to the inaccuracy in the measurement of initial current or chloride concentration.

When Eq. (6) is fitted to the data in Fig. 11, the "crack geometry factor" β_{cr} may be obtained. The β_{cr}value obtained from this study is 0.087 for best fit with lower bound of 0.067 and upper bound of 0.206 as shown in Fig. 13. In other words, the diffusion coefficient at crack is around 0.06–0.2 times the diffusion coefficient of chloride ions in free solutionD_0. Gerard and Marchand [14] report that the tortuosity ranges from 2 to 5 in most cases, and this means that the crack geometry factor, the reciprocal of the tortuosity, is 0.2–0.5 which is

Table 3
Measured rates of chloride concentration change and diffusion coefficients for various test variables.

Specimen ID	crack widths [μm]	$\lvert\Delta c/\Delta t\rvert$ [$\times 10^{-10}$ mol/cm³/s]				$\lvert\Delta(\ln c)/\Delta t\rvert$ [$\times 10^{-7}$ 1/s]		D_{eq} [$\times 10^{-8}$ cm²/s]				
		Upstream		Downstream		Upstream		Upstream		Downstream		Average
		#1	#2	#1	#2	#1	#2	#1	#2	#1	#2	
S15	133.61	1.523	1.587	2.261	2.920	4.917	5.259	2.058	2.202	3.287	4.059	2.901
S21	133.27	1.217	0.784	1.394	0.766	4.211	2.392	1.763	1.002	1.979	0.964	1.427
S30	0.00	0.690	0.749	0.619	0.637	2.292	2.541	0.960	1.064	0.831	0.869	0.931
	14.79	0.714	0.646	0.741	0.513	2.618	2.262	1.108	0.957	1.123	0.746	0.983
	30.21	0.654	0.683	0.687	0.671	2.190	2.298	0.936	0.983	0.961	0.947	0.957
	57.07	0.623	0.841	0.607	0.999	2.051	3.114	0.877		0.837		0.857
	81.58	0.661	0.636	0.679	0.617	2.217	2.059	0.948	0.880	0.912	0.803	0.886
	111.12	0.750	0.752	0.725	0.774	2.752	2.657	1.177	1.136	1.059	1.089	1.115
	155.43	0.599	0.768	0.751	0.782	2.128	2.850	0.910	1.219	1.052	1.126	1.077
	206.46	0.761	0.675	0.853	0.968	2.753	2.467	1.177	1.055	1.311	1.450	1.248
S30F20	121.52	0.502	0.528	0.047	0.160	1.410	1.507	0.590	0.631	0.054	0.188	0.366
S30G13	110.45	0.842	0.858	0.471	0.668	3.050	3.080	1.277	1.289	0.693	0.969	1.057

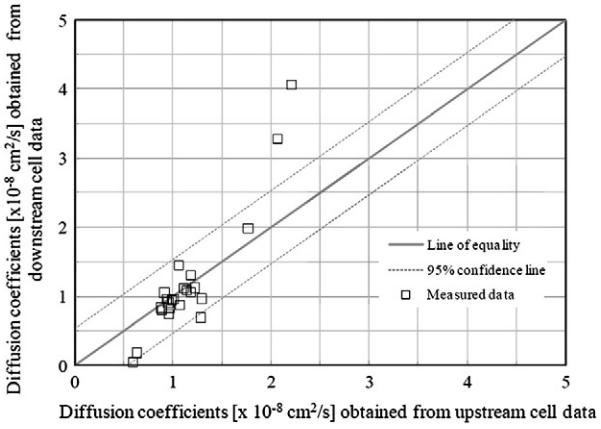

Fig. 10. Comparison of diffusion coefficients obtained from upstream and downstream cell data.

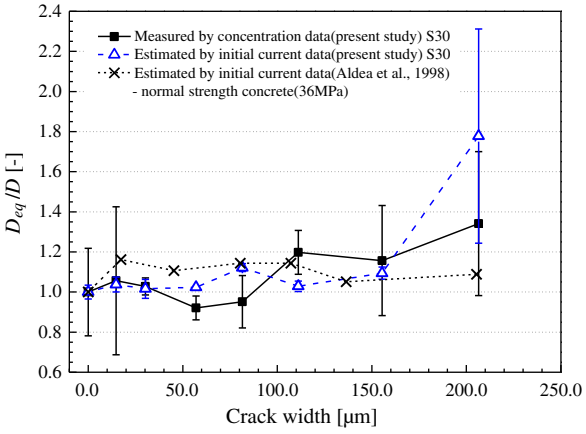

Fig. 12. Comparison of diffusion coefficients obtained from present migration test and those estimated based on initial current data.

somewhat higher than the values obtained in this study. More experimental data may be necessary in the future to evaluate the crack geometry factors for various conditions.

Based on the results in the present study, when fine continuous cracks are densely formed in one direction on the surface of actual concrete structures, the equivalent diffusion coefficients of cracked zone may be evaluated, similarly to Eq. (6), as

$$\frac{D_{eq}}{D} = 1 + \frac{\left(w_{cr} - w_{cr,t}\right)\beta_{cr}}{l_{cr}}\frac{D_0}{D} \tag{11}$$

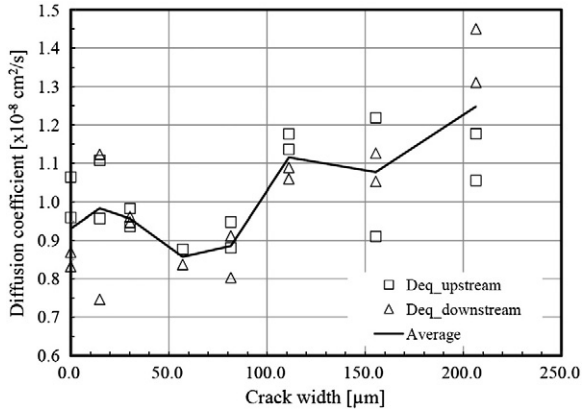

Fig. 11. Diffusion coefficients according to crack widths obtained from present tests.

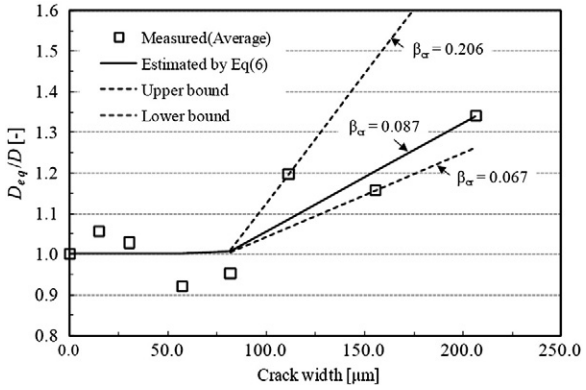

Fig. 13. Relationship between relative diffusion coefficients and crack widths according to crack geometry factor.

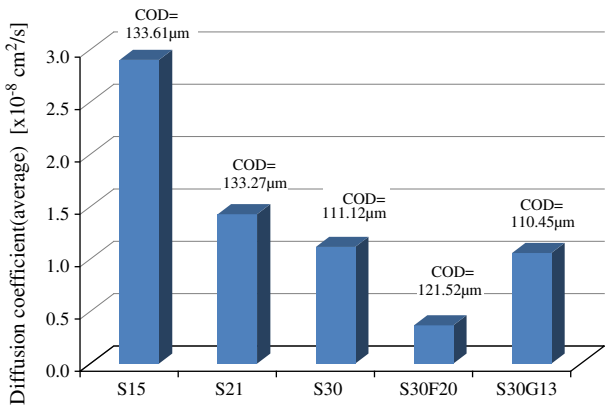

Fig. 14. Comparison of diffusion coefficients according to concrete strength (S15, S21, and S30), addition of fly ash (S30F20) and maximum aggregate size (S30G13).

where l_{cr} is the average crack spacing [m]. However, if cracks are formed sparsely, Eq. (11) may lead to some errors since chloride ingress may be concentrated on crack itself. In this case, diffusion of crack itself should be focused on and cracks can be dealt as a straight channel for diffusion with diffusion coefficient of $\beta_{cr}D_0$. A 2-D or 3-D analysis of ionic diffusion may provide more accurate prediction of chloride penetration at cracked concrete [28,29].

5.4. Effect of concrete strength, addition of fly ash and maximum aggregate size

Fig. 14 shows the effect of concrete strength, fly ash addition and maximum aggregate size on the diffusion coefficient of cracked concrete at the similar crack width values. One can easily find in Fig. 14 that the diffusion coefficient decreases with an increase of concrete strength, and the addition of fly ash decreases further the diffusion coefficient at the similar crack widths. These trends are similar to that in uncracked concrete. This means that the cracking did not alter the effect of the strength and fly ash addition on the transport properties at least up to the crack width of around 110–130 μm, and hence the diffusion of uncracked part still controls the diffusion coefficient in these cases of lower crack width.

It can be also seen that the maximum aggregate size has little influence on the diffusion coefficient of cracked concrete for the crack width less than about 110 μm as shown in Fig. 14. Namely, the diffusion coefficient of the concrete with the maximum aggregate size of 13 mm (S30G13) is almost the same as that of the concrete with the maximum aggregate size of 25 mm (S30) at the crack width of about 110 μm (see Fig. 14).

Further future studies are necessary to establish the effects of concrete strength and maximum aggregate size on the diffusion properties of cracked concrete, especially for wide ranges of crack widths.

6. Conclusions

In this study, the diffusion coefficients of cracked concretes according to different crack widths have been studied. Major test variables include crack width and concrete strength. The effects of fly ash addition and maximum aggregate sizes were also studied. The diffusion coefficients of cracked concretes have been measured by steady-state migration test. The following conclusions were drawn from the present study.

(1) The present study indicates that the diffusion coefficients obtained from the upstream cell in the steady-state migration tests are almost the same as those measured from the downstream cell. Therefore, it is more efficient and time-saving to use the chloride concentration data in the upstream cell, without loosing the accuracy of measurement of diffusion coefficient in the steady-state migration test.

(2) The diffusion coefficients of concrete do not increase with increasing crack widths up to the so-called "threshold crack width," while, over this threshold value, the diffusion coefficients start to increase. The threshold crack width is found to be around 80 μm based on the present test data, which is a little bit larger than, but close to around 55 μm in the previous research.

(3) A parallel composite model was devised to identify the diffusion coefficient of cracked concrete and the "crack geometry factor" was introduced in the model.

(4) A linear relationship between crack width and diffusion coefficient was established. Based on the present test data, this relationship is found reasonable and the crack geometry factor ranges from 0.067 to 0.206.

(5) The present study shows that the diffusion coefficient decreases with an increase of concrete strength at lower crack width values. The addition of fly ash also decreases the diffusion coefficient. These phenomena are similar to uncracked concrete. Thus it is inferred that concrete strength (up to 30 MPa) and addition of fly ash (up to 20% replacement) do not have a significant influence on the crack geometry factor.

(6) Within a limited test data on the maximum aggregate size, it was found that the diffusion coefficient of concrete with the maximum aggregate sizes of 13 mm is similar to that for the maximum aggregate sizes of 25 mm, which indicates that the aggregate size has little influence on the diffusion coefficient of cracked concrete.

It is expected that the results obtained from the present study may be applied to the realistic prediction of chloride penetration into concrete structures, considering the effect of crack on the diffusion coefficients in the durability design of new concrete structures as well as the estimation of residual service life of existing structures.

References

[1] B.H. Oh, S.Y. Jang, Prediction of diffusivity of concrete based on simple analytic equations, Cement and Concrete Research 34 (3) (2004) 463–480.
[2] B.H. Oh, S.Y. Jang, Effects of material and environmental parameters on chloride penetration profiles in concrete structures, Cement and Concrete Research 37 (1) (2007) 47–53.
[3] B.H. Oh, B.S. Jang, Chloride diffusion analysis of concrete structures considering the effects of reinforcements, ACI Materials Journal 100 (2) (2003) 143–149.
[4] B.H. Oh, S.Y. Jang, Experimental investigation of the threshold chloride concentration for corrosion initiation in reinforced concrete structures, Magazine of Concrete Research 55 (2) (2003) 117–124.
[5] C. Andrade, Calculation of chloride diffusion coefficients in concrete from ionic migration measurements, Cement and Concrete Research 23 (3) (1993) 724–742.
[6] T. Zhang, O.E. Gjørv, An electrochemical method for accelerated testing of chloride diffusivity in concrete, Cement and Concrete Research 24 (8) (1994) 1534–1548.
[7] A.V. Saetta, R.V. Scotta, R.V. Vitaliani, Analysis of chloride diffusion into partially saturated concrete, ACI Materials Journal (Sep.–Oct., 1993) 441–451.
[8] K.A. Snyder, C. Ferraris, N.S. Martys, E.J. Garboczi, Using impedance spectroscopy to assess the viability of the rapid chloride test for determining concrete conductivity, Journal of Research of the National Institute of Standards and Technology 105 (4) (2000) 487–509.
[9] L. Tang, Chloride transport in concrete — measurement and prediction, Publication P96:6, Division of Building Materials, Chalmers University of Technology, Göteborg, Sweden, 1996.
[10] O. Truc, J.P. Olivier, M. Carcasses, A new way for determining the chloride diffusion coefficient in concrete from steady-state migration test, Cement and Concrete Research 30 (2000) 217–226.
[11] C.-M. Aldea, S.P. Shah, A. Karr, Permeability of cracked concrete, Materials and Structures 32 (1999) 370–376.
[12] C.-M. Aldea, S.P. Shah, A. Karr, Effect of cracking on water and chloride permeability on concrete, Journal of Materials in Civil Engineering, ASCE (August, 1999) 181–187.
[13] R. Gagné, R. Francois, P. Masse, Chloride penetration testing of cracked mortar samples, in: N. Banthia, et al., (Eds.), Proc. of 3rd International Conference on Concrete under Severe Conditions, The University of British Columbia, Vancouver, Canada, 2001, pp. 198–205.
[14] B. Gérard, J. Marchand, Influence of cracking on the diffusion properties of cement-based materials, Part I: influence of continuous cracks on the steady-state regime, Cement and Concrete Research 30 (2000) 37–43.
[15] B. Gérard, D. Breysse, A. Ammouche, O. Houdusse, O. Didry, Cracking and permeability of concrete under tension, Materials and Structures 29 (1996) 141–151.

[16] B. Gérard, H.W. Reinhardt, D. Breysse, Measured transport in cracked concrete, in: H.W. Reinhardt (Ed.), Penetration and Permeability of Concrete: Barriers to Organic and Contaminating Liquids, E&FN SPON, U.K., 1997, pp. 265–324.
[17] S. Jacobsen, J. Marchand, L. Boisbert, Effect of cracking and healing on chloride transport in OPC concrete, Cement and Concrete Research 26 (6) (1996) 869–881.
[18] K. Wang, D.C. Jansen, S.P. Shah, Permeability study of cracked concrete, Cement and Concrete Research 27 (3) (1997) 181–393.
[19] P. Locogne, M. Massat, J.P. Ollivier, C. Richet, Ion diffusion in microcracked concrete, Cement and Concrete Research 22 (1992) 431–438.
[20] A. Konin, R. François, G. Arliguie, Penetration of chlorides in relation to the microcracking state into reinforced ordinary and high strength concrete, Materials and Structures 31 (1998) 310–316.
[21] R. François, G. Arliguie, Effect of microcracking and cracking on the development of corrosion in reinforced concrete members, Magazine of Concrete Research 51 (2) (1999) 143–150.
[22] C. Tognazzi, J.P. Ollivier, M. Carcassess, J.M. Torrenti, Couplage fissuration–dégradation chimique des matériaux cimentaires: Premiers résultats sur les propriétés de transfert, in: Ch. Petit, G. Pijaudier-Cabot, J.M. Reynouard (Eds.), Ouvrages, géomatériaux et interactions, Hermès, Paris, 1998, pp. 69–84, (in French).
[23] W. Wittke, Rock mechanics: theory and applications with case histories, Springer, Berlin, 1990.
[24] CEB-FIP Model Code 90, CEB, Thomas Telford, U.K., 1993
[25] E.J. Garboczi, Permeability, diffusivity, and microstructural parameters: a critical review, Cement and Concrete Research 20 (4) (1990) 591–601.
[26] Handbook of Chemistry and Physics, 81th ed.CRC Press, Washington, D.C., 2000.
[27] ASTM C 1202, Standard test method for electrical indication of concrete's ability to resist chloride ion penetration, Annual Book of ASTM Standards, American Society for Testing and Materials, 2005.
[28] O.B. Isgor, A.G. Razaqpur, Finite element modeling of coupled heat transfer, moisture transport and carbonation processes in concrete structures, Cement & Concrete Composites 26 (2004) 57–73.
[29] J. Carmeliet, J.-F. Delerue, K. Vandersteen, S. Roels, Three-dimensional liquid transport in concrete cracks, International Journal for Numerical and Analytical Methods in Geomechanics 28 (2004) 671–687.